27

Measurement of Lipid Forces by X-Ray Diffraction and Osmotic Stress

Horia I. Petrache, Daniel Harries, and V. Adrian Parsegian

Summary

Lipid suspensions in aqueous solutions most often form multilamellar vesicles of uniformly spaced bilayers. Interlamellar spacing is determined by the balance of attractive van der Waals (charge fluctuation) and repulsive forces. This balance of forces, as well as membrane elasticity, can be probed by applied osmotic stress. We describe how osmotic stress can be imposed on multilamellar lipid samples to study lipid interactions.

Key Words: Bending rigidity; cholesterol hydration; membrane fluctuations; osmotic pressure; spontaneous curvature.

1. Introduction

1.1. Interlamellar Forces

Because of mutually induced charge fluctuations, lipid membranes attract one another *(1)*. This charge fluctuation or van der Waals (vdW) force is responsible for the spontaneous formation of stable multilamellar structures: for example myelin sheets in vivo and multilamellar vesicles (MLVs) in vitro *(2–6)*. The vdW force is present regardless of the charged state of constituent lipids. Because attractive vdW interactions are counteracted by repulsive forces *(2)*, this attraction does not lead to the collapse of membrane stacks. Instead, an equilibrium spacing between lamellae is established to create equally spaced multilamellar structures of hundreds of layers. Measured by small-angle X-ray scattering, the interlamellar repeat spacing of neutral membranes made of phosphatidylcholines (PCs) and/or phosphatidylethanolamines (PEs) in aqueous solvents, is on the order of 50–100 Å, depending on acyl-chain composition, temperature, and other thermodynamic variables *(2)*. This repeat spacing represents the sum of membrane thickness and interlamellar water layer, with roughly equal contributions *(7)*.

Except for purely electrostatic forces, repulsive forces between membranes have an entropic origin. First, the work needed to remove hydrating waters opposes the membrane approach *(2)*. By direct measurement, this force (or free energy penalty) has been shown to be exponential with a decay length of about 2 Å. Second, an additional repulsive force, also of entropic origin, is due to confinement of membrane undulations *(8)*. As measured experimentally *(9)*, this force is also exponential with a decay length of 5–6 Å. The mutual restriction of thermally driven undulation (bending fluctuations) of approaching membranes incurs an entropic penalty. This penalty is proportional to a bending rigidity (elasticity), K_C, and mean-square fluctuations, σ. If the force (per area) needed to push membranes together is measured, the

From: *Methods in Molecular Biology, vol. 400: Methods in Membrane Lipids*
Edited by: A. M. Dopico © Humana Press Inc., Totowa, NJ

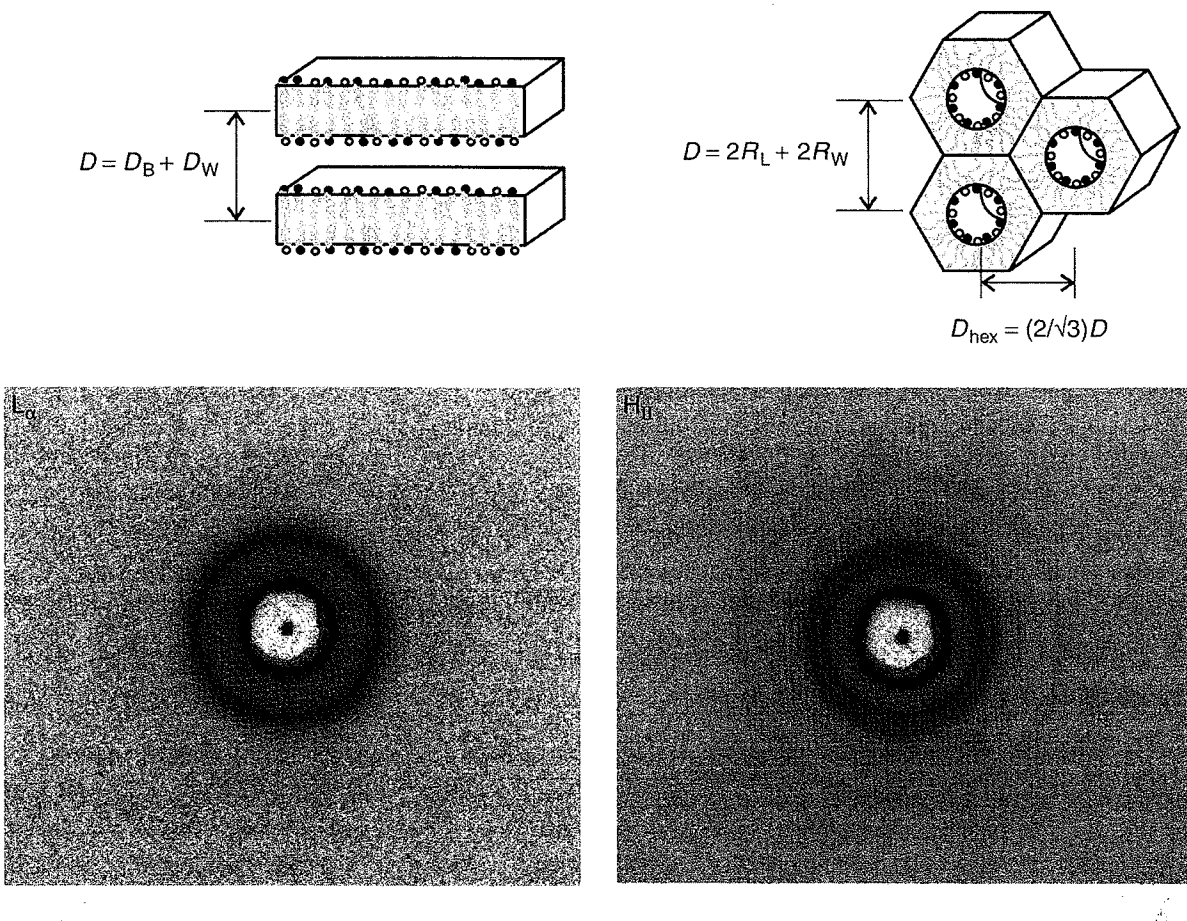

Fig. 1. X-ray scattering from multilamellar (L_α) DMPC and inverted hexagonal (H_{II}) DOPE, both fully hydrated at 35°C. Scattering rings of DMPC are equally spaced and reflect the regular spacing between stacked bilayers. The X-ray rings of DOPE index as 1, $1/\sqrt{3}$, 1/2, $1/\sqrt{7}$, . . . and reflect the honeycomb-like positioning of water cylinders in the H_{II} phase.

"spring constant" that restricts thermal motion is determined. How can it be done? By removing interlamellar water (i.e., by dehydrating the MLVs) using osmotic stress ***(10)***. The chapter describes this approach.

1.2. X-Ray Images of Lipid Phases

Depending on acyl-chain and headgroup composition, lipids can form not only lamellar structures but also hexagonal phases **(Fig. 1)**. Lipids with saturated acyl chains and PC headgroups tend to form bilayer phases at physiological temperatures. Conversely, lipids with unsaturated chains and PC (demethylated PC) tend to form inverse hexagonal phases. The 14-carbon disaturated dimyristoylphosphatidylcholine (DMPC) and the monounsaturated 18-carbon dioleoylphosphatidylethanolamine (DOPE) are common representatives of each class. DOPE has a negative spontaneous curvature and forms an inverted hexagonal phase when fully hydrated. DMPC, having a much smaller spontaneous curvature, forms a lamellar phase. The geometry of lipid aggregates, and corresponding X-ray pictures are shown in **Fig. 1**. Uniform scattering rings are obtained owing to random, "powder" orientations of lipid suspensions in the X-ray beam. The lattice (repeat) spacings are determined from the position of these rings. For lamellar structures, the rings are equally spaced and indexed simply as 1, 1/2, 1/3, ... (1/*h*,

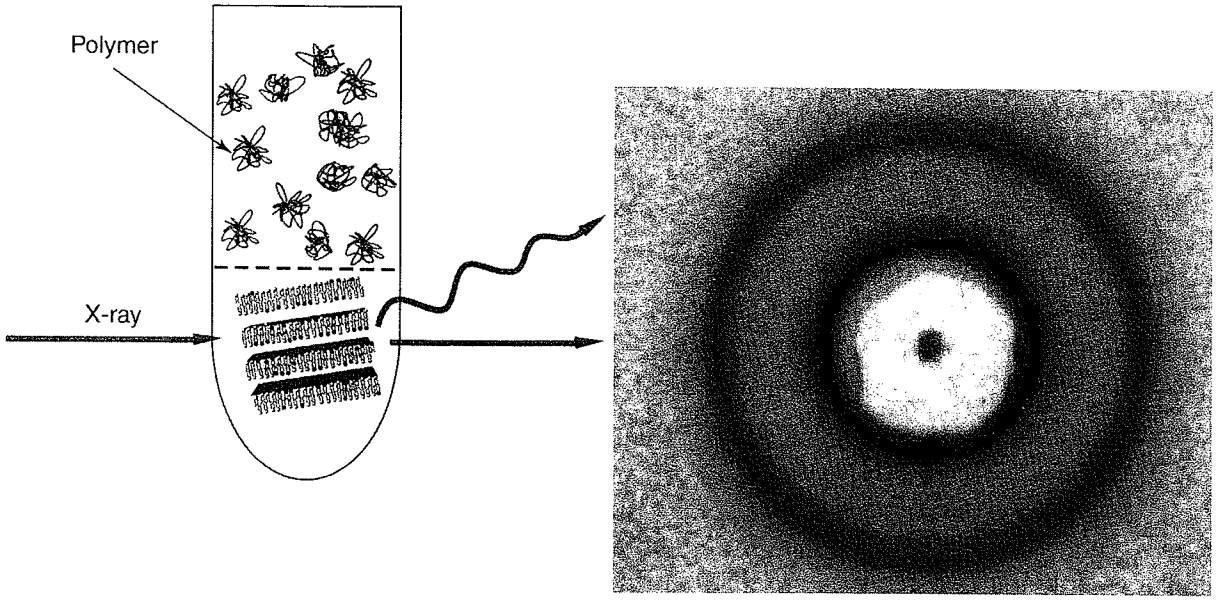

Fig. 2. Schematic of a multilamellar lipid domain under osmotic stress. Using large molecular stressors (polymers) that are excluded from the interlamellar space eliminates the need for a dialysis membrane (dashed line). A typical scattering pattern obtained from randomly oriented domains (MLVs) is shown.

$h = 1, 2, 3, \ldots$), whereas for the H_{II} phase the indexing is 1, $1/\sqrt{3}$, 1/2, $1/\sqrt{7}$, ... ($1/(h^2 + hk + k^2)^{1/2}$, $h, k = 0, \pm1, \pm2, \ldots$).

For fully hydrated DMPC in water at 35°C, the interlamellar repeat spacing is D = 63 Å, which is decomposed into a bilayer thickness D_B = 44 Å, and a water spacing D_W = 19 Å (**Fig. 1**). For DOPE, with a hexagonal lattice spacing D_{hex} = 64 Å, D = 74 Å, with $2R_L$ = 36 Å, and $2R_W$ = 38 Å. The water content measured by D_W or R_W, can be reduced by osmotic stress. Although this chapter focuses on lamellar structures, the experimental techniques described apply to hexagonal structures as well.

2. Methods

2.1. Overview of the Osmotic Stress Method

The osmotic stress technique has become a popular tool for investigating the forces acting between lipid bilayers, as well as between other macromolecules *(11,12)*. Osmotic action represents the addition or removal of solvent molecules, most often water. Imposed by the presence of solutes (osmolytes), osmotic pressure acts on the water that hydrates the macromolecular or lipid aggregate. Glycerol, dextran, polyethylene glycol (PEG), and even common salts can be used as osmolytes *(13–18)*. Typically, the method uses either a semipermeable membrane (dialysis bag) that confines the large osmolytes yet allows water (and small osmolytes) to pass, or uses large solutes that are strongly excluded from the lipid aggregates, such as high molecular weight polymers (e.g., PEG) for which a dialysis membrane is not needed. By competing with lipid for available water, osmolytes reduce the equilibrium separation between lipid bilayers. Once equilibrated, the spacing between lipid bilayers at a specified osmotic pressure can be determined using X-ray scattering. This allows to measure the equation of state (force vs separation curves) for the bilayer stack *(9,19–21)*. **(Fig. 2)**.

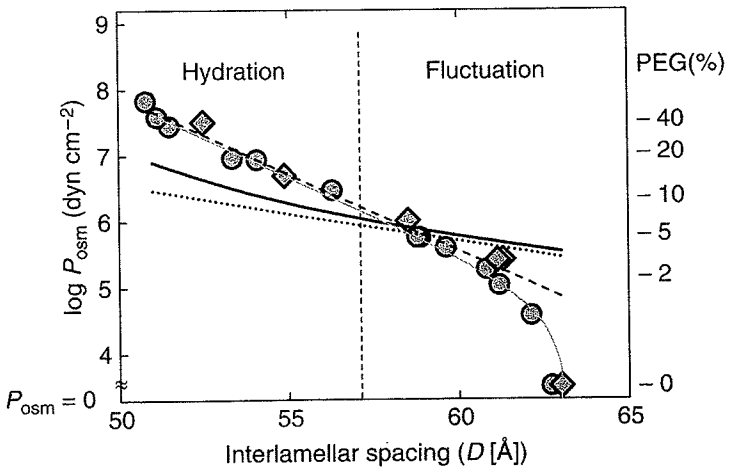

Fig. 3. Osmotic pressure vs interlamellar spacing for DMPC at 30°C (circles) and 35°C (diamonds), and theoretical decomposition into vdW (solid line), hydration (dashed), and fluctuation repulsion (dotted). Two regimes are distinguished: at low osmotic pressure wherein repulsion is dominated by fluctuations; and at high pressure wherein repulsion is mainly because of hydration. Reference PEG concentrations (MW = 20,000 g/mol) are shown on the right. The osmotic pressure vs PEG concentration is measured separately with a vapor pressure osmometer. Figure adapted from **ref. *41***.

2.2. Measurement of Interlamellar Forces

Results from an osmotic pressure experiment of (net neutral) DMPC multilayers are shown in **Fig. 3**. The interlamellar repeat spacing (D) from a series of DMPC samples equilibrated with PEG solutions of various concentrations are plotted for the corresponding pressures P_{osm}. Because relevant osmotic pressure values span many orders of magnitude data are typically plotted on a log scale. Note that the fully hydrated spacing corresponds to zero osmotic pressure and is arbitrarily placed on the log scale. Reference PEG concentrations (mylar window [MW] = 20,000 g/mol) are shown on the right. Osmotic pressure tables from Peter Rand and coworkers can be found at www.brocku.ca/researchers/peter_rand (also mirrored at lpsb.nichd.nih.gov/osmotic_stress.htm).

Because samples are in equilibrium, the applied osmotic pressure is exactly counterbalanced by the net interbilayer force. This force is, to a first approximation, a simple sum of the attractive and repulsive interactions. Interaction energies are given below ***(9)***.

$$F(D_W) = -\frac{H}{12\pi D_W^2} + P_h \lambda e^{-D_W/\lambda} + \left(\frac{k_B T}{2\pi}\right)\frac{1}{K_C \sigma^2} \qquad (1)$$

The first term represents the vdW attraction with interaction strength quantified by the Hamaker parameter H, typically in the order of 1–2 $k_B T$. The second term represents the hydration repulsion with amplitude P_h and decay length λ. The last term represents the undulation (Helfrich) force depending on membrane bending rigidity (K_C) and mean-square fluctuation (σ); for measurement of σ, readers should *see* **refs. *9*** and ***22***. In **Eq. 1**, the derivative of free energy with respect to the interlamellar water spacing (D_W) equals the applied osmotic stress:

$$P_{osm} = -\frac{dF(D_W)}{dD_W}$$

Two distinct regimes are outlined in **Fig. 3**. At low applied pressures of a few atmospheres, membrane fluctuations serve as the dominant repulsive term, and the hydration force can be neglected. In contrast, at higher pressures, hydration acts as the main repulsive term counteracting vdW attraction. Therefore, it should be expected that low applied osmotic pressures mainly suppress repulsion owing to fluctuations *(9)*.

2.3. Work Done by Osmotic Stress

The applied osmotic pressure is in fact related to the amount of work required to change the separation between bilayers *(23)*. It is useful to realize that this work is the reversible work (or free energy) required to remove water from between the lipid layers and into a reservoir of pure water, conveniently expressed in terms of water's chemical potential (μ_w) that is related to water activity (a_W) through

$$\mu_W = \mu^0 + RT \ln a_W$$

where T is the absolute temperature and R is the gas constant; μ^0 is a reference "standard" chemical potential. The molar free energy of water in the lipid phase measured with respect to pure water is:

$$\Delta\mu_W = \mu_W - \mu_W^{bulk}$$

Because lipids form large aggregates that negligibly modify water's chemical potential ($\Delta\mu$W) is also simply a measure of the osmotic pressure (Posm) of the water in lipid solution:

$$\Delta\mu_W = -V_W P_{osm}$$

where V_W is the volume of a water molecule (~30Å^3 at 30°C). Therefore, the incremental work needed to change membranes' spacing to release a small volume of water dV, translates to the chemical potential of water at that spacing,

$$\Delta\mu_W dn = -V_W P_{osm} d(V / V_W) = -P_{osm} dV$$

or expressed in terms of D-spacing per lipid with headgroup area A

$$\Delta\mu_W dn = -AP_{osm} dD.$$

At equilibrium, the net flow of water from the lipid phase to the bath is zero; the cost of removing water from one phase must equal the gain of adding it to the other, so that the force per unit area is:

$$P_{osm} = -dF / dD_W.$$

2.4. How to Impose and Measure Osmotic Stress

A simple and often practical way to change water activity in a stack is to limit the amount of available water (so-called gravimetric method) *(24)*. The stack will incorporate as much water as available (if this amount is less than the amount needed for maximal swelling). Once water is incorporated between lipid membranes it will generally be harder to remove than from a pure water phase. Measuring the vapor pressure in the gas phase over the equilibrated

multilayers directly assesses this difference *(2)*. It is found that the vapor pressure of water is lower than over a pure water phase (increased osmotic pressure), indicating that added free energy is required to draw water from the lipid phase. The chemical potential of water is lower in the lipid phase compared with pure water.

The complementary strategy to limit the amount of water in the system is to equilibrate the aggregate against a bulk solution (bath) with a known osmotic pressure, allowing only water to move between the two phases *(2)*. For example, water can equilibrate through the vapor phase connecting the system and the bath (hydration chamber principle) *(17,25,26)*, or else through a partition allowing water but not solute to pass (dialysis). Here, any (nonvolatile) solute can be used as the osmotic stressor. Some solutes are so strongly excluded from the lipid phase that they can effectively serve as osmotic stressors even in the absence of a physical partition between the MLVs and the bath. This has been verified experimentally by comparing the interbilayer spacing equilibrated against high molecular weight PEG and other polymers, with and without partition (dialysis bag). However, care must be taken to ensure that solutes are indeed completely excluded. In particular, when smaller solutes are used or when several solutes are present in solution, the solutes can sometimes partition between the bath and aggregate phases as well, thus changing the water chemical potential whereas not always exerting their full osmotic effect *(27–30)*. For example, an added solute may happen to partition equally between the bath and lipid phase; in this case, the solute will exert no net osmotic stress on the bilayer stack, even though it significantly alters water activity.

A typical experiment starts with preparation of PEG solutions of known concentrations. Next, the osmotic pressure for each solution is measured, for example, by vapor pressure osmometry. This method gives an accurate determination of osmotic pressures in the range of just a few to almost 100 atm (~93% relative humidity [RH], *see* **Subheading 2.5.**). Finally, dry lipid is hydrated in excess PEG solutions and left to equilibrate. As the lipid hydrates by taking water from the PEG solution, PEG concentration in the bath increases. However, for small amount of lipid (e.g., 10 mg dry lipid/1 mL PEG solution), this perturbation can be neglected. In different situations, including the case of solute mixtures that can be partially incorporated into the MLVs, the osmotic pressure of the bath should be measured after MLVs have equilibrated. For some widely used solutes such as PEG and dextran, osmotic pressure values vs polymer concentration are available online at www.brocku.ca/researchers/peter_rand and lpsb.nichd.nih.gov/osmotic_stress.htm.

2.5. Osmotic Stress Units

The action of osmolytes can be reported either in pressure units (N/m^2 in SI and dyn/cm^2 in CGS) or corresponding RH with the equation

$$P_{osm} = -(k_B T / V_W) \log \mathrm{RH}$$

where V_W represents the volume of a water molecule (~30Å^3 at room temperature). At room temperature, 1 atm then corresponds to RH = 99.9%, 50 atm to RH = 98%, and 100 atm to RH = 93%. In this range of pressures, one has $P_{osm} \cong (1.4 \times 10^9)$ (1–RH).

3. Sample Preparation

Most lipids are now available in high purity (>99%) from commercial sources such as Avanti Polar Lipids (Alabaster, AL) and Sigma-Aldrich (St. Louis, MO). Lipids can be ordered

either in powder form or dissolved in chloroform. For work with unoriented MLVs, dry lipids between 3 and 15 mg of per sample (vial) have been used with the steps given below. Note that the equilibration time needed to obtain a homogeneous lipid sample can vary significantly with the lipid type and solvent used. Variations of the protocol are strongly recommended. With many suggestions from Stephanie Tristram-Nagle, Nola Fuller, Peter Rand, and Don Rau; the following procedures worked very well.

3.1. MLVs for X-Ray Scattering

1. Remove lipid bottle from freezer and let it equilibrate at room temperature before opening, to minimize hydration from air.
2. Use a spatula to transfer 3–15 mg of dry lipid into 1–2 mL plastic vials (*see* **Fig. 4**) and weigh. Because hydration is important, using vials provided with *O*-ring screw-caps is preferred. Beware that dry lipids can easily acquire electrostatic charge and fly off the spatula. Some others, such as DOPC, are sticky and require brushing of spatula on the inner walls of the vial to get the lipid off.
3. Add between 850 µL and 1 mL of premade solvent containing one or more of pure water, salt solutions, PEG solutions, and pH buffers.
4. Shake vial gently to dissolve all lipid powder.
5. Thermocycle the samples between 0°C and 5° to 10°C above the lipid melting temperature. Melting temperatures can be found in the online Lipidat database www.ldb.chemistry.ohio-state.edu. PC lipids with saturated chains melt at about 4, 24, 41, and 55°C for 12, 14, 16, and 18 carbons, respectively *(31)*. Phosphatidylserine (PS) and PE lipids melt about 10–20°C higher *(32,33)*. Lipids with unsaturated chains usually melt at lower temperatures. Samples can be shaken by hand or vortexed gently between temperature jumps from low-to-high and back, held at each temperature for about 5–10 min, and the cycle should be repeated at least three times. In principle, automatic thermocycling could also be used.
6. Store samples at 4°C for 48 h. Sedimentation of MLVs occur as shown in **Fig. 4**.
7. Before measurement, let vial equilibrate at the temperature of the measurement for 30 min to 2 h, with longer waiting times for more viscous samples. Gentle shaking or vortexing can also be performed to homogenize the samples. Centrifuge vials at low speed to repellet the MLVs. Note that, depending on lipid and solvent density, the MLVs can either sink or float *(34,35)*. In most cases the MLV aggregate is visible by eye even when not fully opaque.

3.2. Lipid Mixtures

1. Use chloroform or customized organic solvents (*see* Chapter 5) to codissolve measured quantities of lipid. Use standard glass test tubes.
2. Evaporate solvent under chemical hood using either an evaporator or manually by flowing nitrogen or argon gas. After evaporation, the lipid should form a thin film on the glass walls. Best results are obtained with lipid quantities less than 50 mg per test tube.
3. Cover test tubes with parafilm and punch needle holes for further evaporation. Place under high vacuum for at least 4 h or overnight if the sample is chemically stable.
4. There are many options at this point. Samples can be scraped off the glass, transferred into plastic vials, and hydrated according to the protocol in **Section 3.9**. Alternatively, samples can be hydrated in the original test tubes, thermocycled, and stored as such for short period. Seal with parafilm. Another alternative is to resuspend the lipid film in hexane or water and then lyophilize. This is done by quick freezing in dry ice followed by evaporation under high vacuum. After lyophilization, the fluffy powder can be hydrated as done previously.

3.2.1. Complications

The most delicate step is the weighing of dry lipid and the pipetting of small chloroform solution volumes. Errors in the estimate of lipid fractions will occur. It is best to deliver the

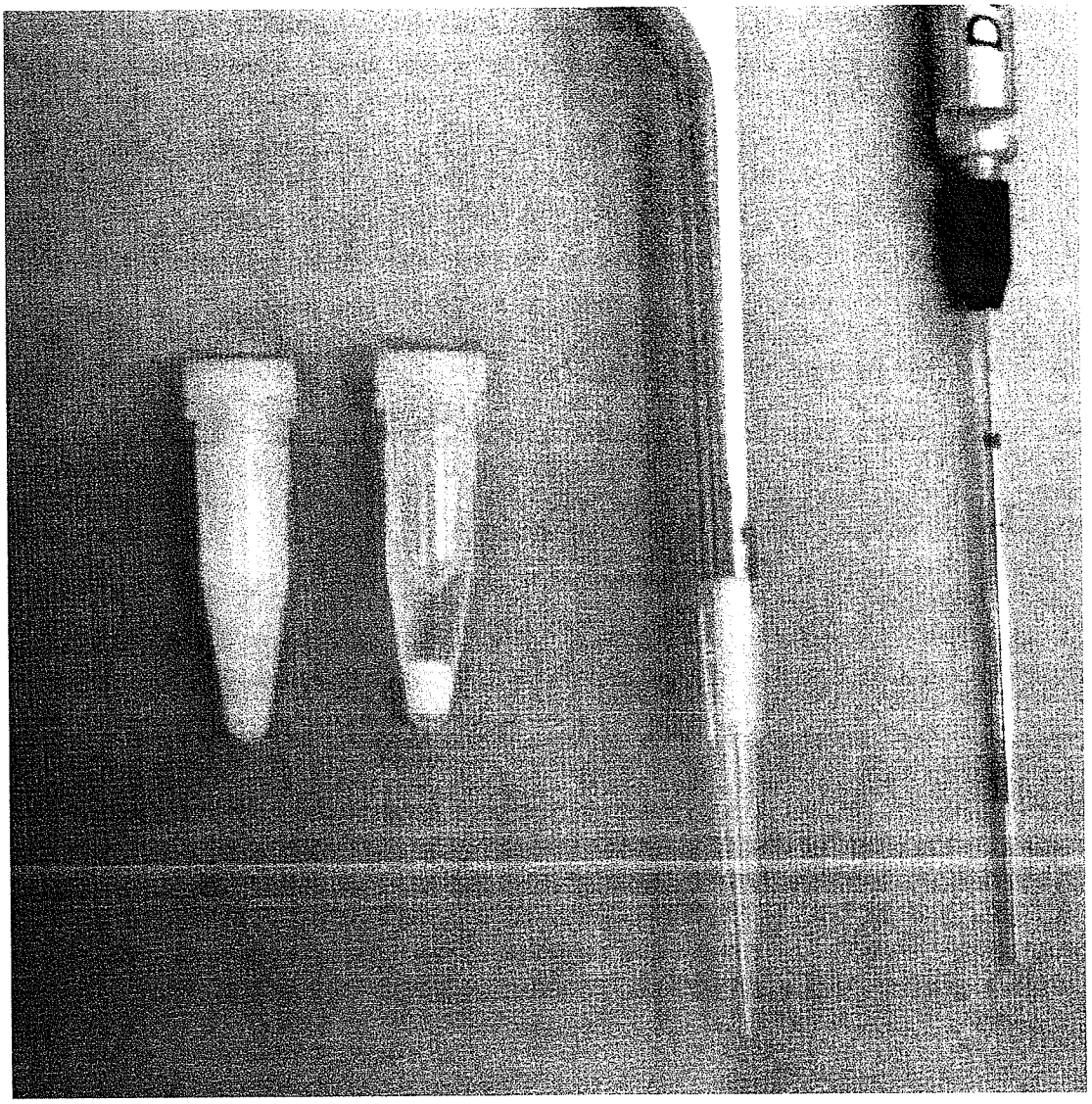

Fig. 4. Visual appearance of MLVs suspensions in aqueous solvents before and after sedimentation. The lipid pellet can be transferred into the sample holder using either a 10–100 μL micropipet, or a positive displacement 10–50 μL capillary pipet for viscous samples.

first chloroform drop on the bottom of test tubes, then the next containing the different lipid very close to it, but do so on the tube wall without touching the previous drop with the pipet tip.

3.3. Loading the X-Ray Sample Holder

3.3.1. The Sample Cell

Traditional sample cells (SCs) originally designed by Vittorio Luzzati and further modified by Peter Rand and coworkers are used. These cells contain a Teflon holder (TH) for the lipid pellet that is sandwiched between two mylar windows as shown in **Fig. 5**. The exact dimensions of the SC and holders are not critical as long as they match. Aluminum cells with a central hole of 2 mm in diameter were used. This central area will sit in the X-ray beam. The X-ray setup includes a matching cell crate sitting on a Peltier device that controls sample temperature. Once properly aligned, this setup allows remounting of the SCs without further adjustment.

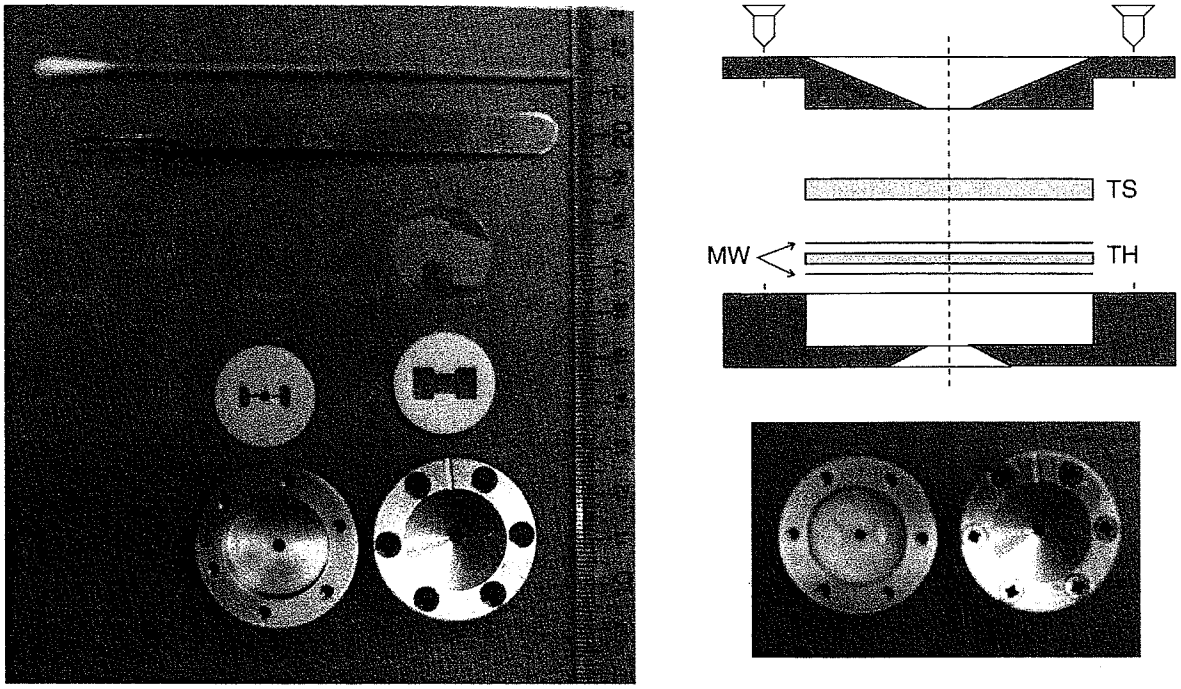

Fig. 5. The SC assembly. The lipid suspension is sequentially loaded into the teflon holder, sandwiched between mylar windows, placed inside the SC, and secured with screws. Tweezers and cotton swabs can be used to manipulate the MWs as described. The SC can be placed in the X-ray beam either way; however, the sample-to-film distance can differ between the two orientations and needs to be checked with a calibrator (e.g., AgBeh with interlamellar repeat spacing $D = 58.4$ Å (*see* **ref. *36***). Because the TS is put systematically on top of TH, the upper (shown) side of the cell is used as the X-ray exit side.

3.3.2. Teflon Holders

Holders are cut from 0.8–1 mm Teflon sheet. A central hole of 2-mm diameter is used to deposit the lipid pellet. Additional cutting can be made to hold extra PEG solution for multiple temperature measurements without reloading the cell.

3.3.3. Mylar Windows

Windows are cut from 100 µm mylar film by using a punch tool. The film is wrapped several times around a piece of cardboard so as to cut through many layers at once. Windows can also be cut by hand because they do not need to be perfectly circular. Before using, windows should be wiped with lens paper to remove dust and lint.

3.3.4. Loading the Sample Cell

1. Prepare a clean Sample cell, Teflon holder, Teflon spacer (TS), and two mylar windows.
2. Apply a thin film of vacuum grease on the TH to insure a good seal with the MWs. Avoid spreading grease on the holder center. If it does happen, grease can be removed using the wooden part of a cotton swab.
3. Using tweezers, stick one MW to one side of the TH (press circularly with the cotton swab), and set the holder inside the SC (**Fig. 5**).
4. Using a pipet, transfer between 10 and 2 µL of lipid pellet into the TH.

5. If the TH has lateral reservoirs, as in **Fig. 5**, fill them with solvent and make sure the solvent drop is continuous from side to side.
6. Using the tweezers, cover the sample with the second MW, avoiding trapping bubbles (slight overloading helps prevent bubbles). For a good seal use the cotton swab to press the mylar gently onto the TH.
7. Place the TS and the cell lid on top. The spacer is only needed if the height of the cell exceeds the width of the TH. Secure the lid with screws.
8. Re-equilibrate the loaded SC at the temperature of the measurement.

3.3.5. Complications

1. In principle, lipids might become contaminated with vacuum grease used to seal the MWs. No indication of such effects have been observed in the studies of PC, PE, and PS lipids at temperatures between 5° and 50°C while in aqueous buffer solutions. If such contamination is suspected, measurements can be done without vacuum grease by relying on a pressure seal between the mylar and Teflon. Dehydration of the sample should then be checked, for example, by repeating the X-ray scan.
2. In the absence of control X-ray data, lipid degradation resulting from oxidation or other chemical reactions should be checked, for example by thin-layer chromatography.

4. The X-Ray Measurement

4.1. A Basic X-Ray Setup

The basic X-ray setup permits quick sample replacement and accurate measurements of interlamellar spacings (**Fig. 6**).

The SC is held in the X-ray beam by sitting in a fixed crate, thermally regulated by a Peltier device, X-ray scattering is recorded on an image plate placed inside a 5 × 4 Fidelity Elite film holder (Fidelity, Sun valley, CA). The original entrance window was removed and replaced with a sheet of black paper usually used to protect photographic film. This paper is opaque at optical wavelengths but transparent to X-rays. To reduce background scattering, the X-ray beam travels between the sample and film through a helium-filled flight path (FP). Helium gas is flown continuously at very low pressure from a helium tank, through the flight path, and bubbled through an oil-filled vial out into the room. A semitransparent beamstop is fixed with double-stick tape on the exit window of the FP, just in front of the film. The shadow of the beamstop is visible in **Fig. 1**.

4.2. X-Ray Measurement and Analysis

Typical exposure times on the machine vary between 20 min and 3 h, depending on the concentration and ordering of MLVs. Fully hydrated samples tend to give weaker scattering than samples under osmotic stress. Phosphor imaging plates are used as detectors and a Fujifilm BAS-2500 plate reader (Fujifilm Life Science, Stamford, CA) capable of 50-μm pixel size. For analysis of X-ray spectra, the software FIT2D by Andy Hammersley (www.esrf.fr/computing/scientific/FIT2D) is very good and easy to use. To calculate the *D*-spacing, the sample-to-film distance is needed. This can be determined using silver behenate (AgBeh) powder as a calibrator. The *D*-spacing of AgBeh is 58.4 Å at room temperature *(36)*. For small angle scattering, the sample-to-film distance is

$$s = \Delta y(D / \lambda)$$

where Δy is the position of the first scattering ring in millimeters, D is the lattice spacing of AgBeh, and $\lambda = 1.54$ Å is the X-ray wavelength (from a Cu anode) (**Fig. 7**).

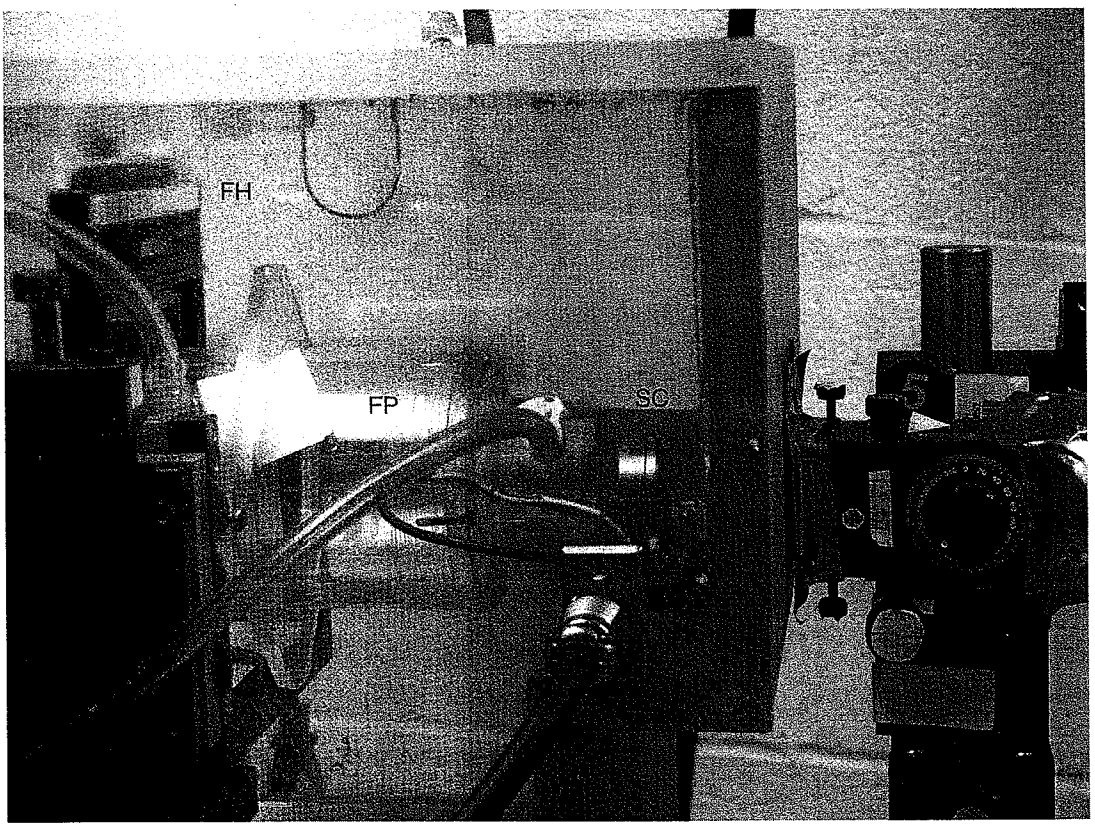

Fig. 6. Sample mounting on an X-ray port. The geometry is fixed. Sample cell, film holder, and flight path sit together inside a plexiglass box that can be oriented as needed to maximize X-ray intensity from the anode and through the focusing mirrors (*see* **ref. *42*** for information on mirror alignment).

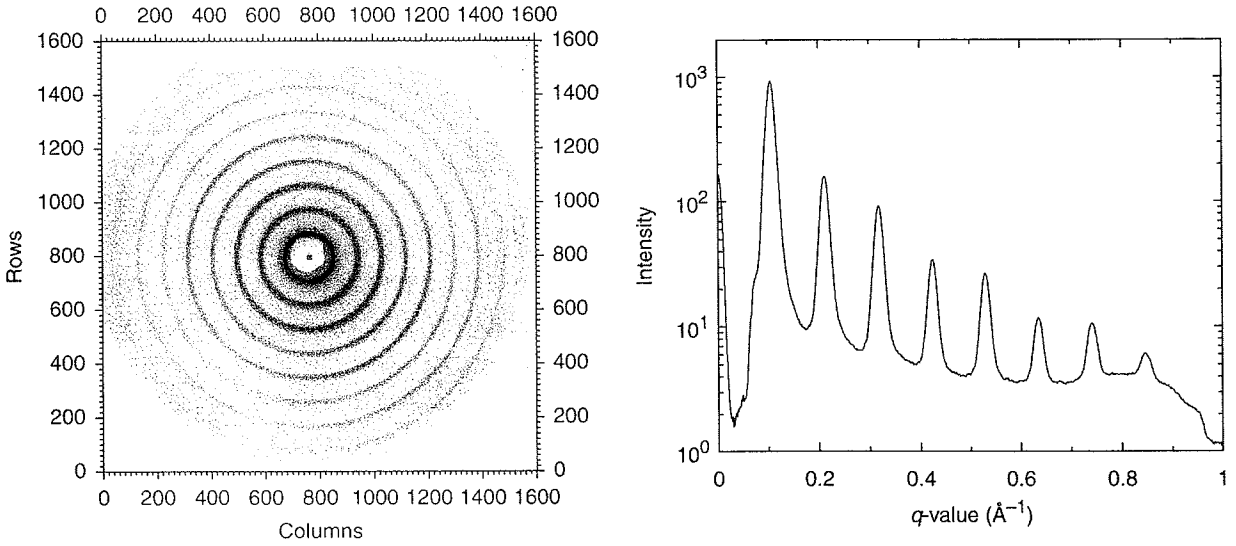

Fig. 7. X-ray scattering from AgBeh powder and radially integrated profile using the program FIT2D available from www.esrf.fr/computing/scientific/FIT2D. The known lattice spacing of 58.4 Å ***(36)*** allows calculation of the sample-to-film distance. AgBeh was kindly provided by Stephanie Tristram-Nagle.

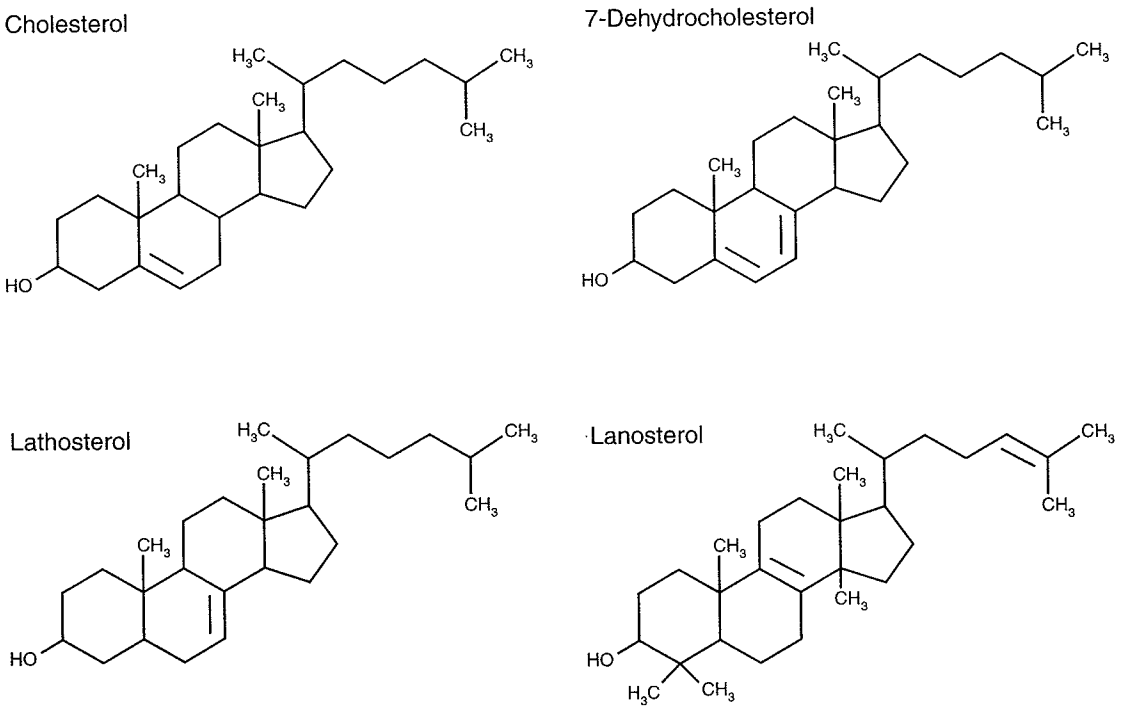

Fig. 8. Chemical structure of cholesterol and some of its metabolic precursors.

5. A Practical Example: Alteration of Membrane Rigidity by Sterols

5.1. A Cholesterol Problem

It is widely believed that an excess of cholesterol leads to atherosclerosis, cardiovascular diseases, and stroke. However, cholesterol deficiency is also dangerous, leading to serious congenital anomalies and mental retardation in newborns. These deficiencies occur when the chain of enzymatic reactions that lead to formation of cholesterol is broken *(37,38)*. Cholesterol precursors, such as the immediate precursor 7-dehydrocholesterol then accumulate in the cell instead of cholesterol. Although cholesterol and its precursors differ only by the number and position of double bonds and methyl groups **(Fig. 8)**, it is found that bilayer rigidity conferred by cholesterol differ significantly from its precursors.

5.2. Applying Osmotic Stress to Sterol-Containing Bilayers

Using the repeat spacing as an indicator of modified interbilayer interaction, the modification of bilayer interactions by addition of sterols can be investigated. As shown in **Fig. 8**, there are marked differences between the effects of sterols on interlamellar repeat spacings at full hydration. For all bilayer compositions, the lamellar repeat spacing increases in the order: cholesterol < lathosterol < 7-dehydrocholesterol < lanosterol. However, differences vanish under only 0.26 atm of osmotic stress (5% PEG solutions, $\log P_{osm} = 5.4$) when fluctuations are suppressed. From the modifications of interlamellar spacings, the modification of bending rigidities have been calculated using **Eq. 1**, as shown in **Fig. 9**.

Differences in sterol effects on membrane rigidity can be rationalized in terms of sterol location within the lipid bilayer. It is expected that sterols introduce an inhomogeneous

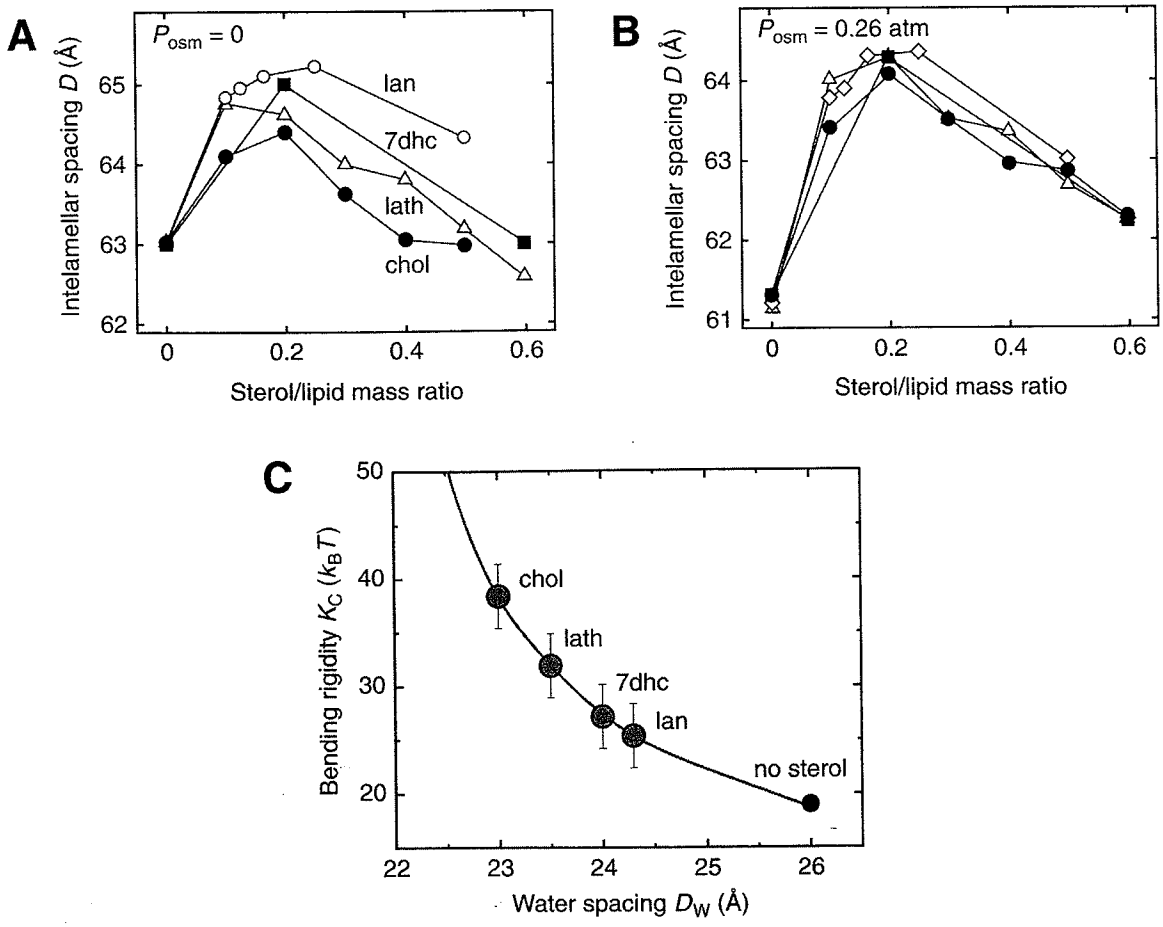

Fig. 9. Interlamellar repeat spacing vs sterol content for DMPC multilayers at 35°C. Differences between sterols measured at full hydration **(A)** vanish when fluctuations are suppressed by mild osmotic stress **(B)**. **(C)** Membrane bending rigidity (K_C) vs equilibrium spacing obtained from **Eq. 1** (solid line). Symbols indicate K_C and D_W measured for 30 mol% sterols. Figure adapted from **ref. *41***.

modification of lateral forces within bilayers. For example, more polar sterols (owing to additional double bonds) might protrude further into the headgroup–water interface than cholesterol, and render the bilayer more flexible. The variation of D with sterol content in **Fig. 8** reflects the phase diagram of DMPC–sterol mixtures. At 35°C, a coexistence region exists between a liquid-disordered phase (with low sterol content) and a liquid-ordered phase (with high sterol content). The steep decline in the D-spacing values starting at a sterol/lipid mass ratio of 0.2 (30% mole sterol) corresponds to the transition to the liquid-ordered phase.

Although many questions regarding lipid–cholesterol interactions still remain, this example demonstrates the versatility of the osmotic stress technique. Used here primarily to analyze interlamellar interactions, osmotic stress also probes interactions within membranes. Because dehydration not only reduces intermembrane separation but also condenses lipids laterally *(23)*, the work of lateral deformation can be measured *(39,40)* and related to forces acting in the membrane plane. Capable of revealing forces with immediate biological relevance, the osmotic stress technique should become the method of choice for investigating interactions between and within membranes.

Acknowledgments

We thank Stephanie Tristram-Nagle, Nola Fuller, Peter Rand, and Don Rau for teaching us the methods in this chapter and much more. This research was supported by the Intramural Research Program of the National Institutes of Health and National Institute of Child Health and Human Development.

References

1. Parsegian, V. A. (2005) *Van der Waals forces: A Handbook for Biologists, Chemists, Engineers, and Physicists*. Cambridge University Press, ISBN 0521547784 (New York, NY)
2. Rand, R. P. and Parsegian, V. A. (1989) Hydration forces between phospholipid bilayers. *Biochim. Biophys. Acta.* **988,** 351–376.
3. Luzzati, V. and Husson, F. (1962) The structure of the liquid-crystalline phases of lipid-water systems. *J. Cell Biol.* **12,** 207–219.
4. Luzzati, V., Reis-Husson, F., Rivas, E., and Gulik-Krzywicki, T. (1966) Structure and polymorphism in lipid-water systems, and their possible biological implications. *Annu. NY Acad. Sci.* **137,** 409–413.
5. Rand, R. P. and Luzzati, V. (1968) X-ray diffraction study in water of lipids extracted from human erythrocytes. *Biophys. J.* **8,** 125–137.
6. Luzzati, V., Benoit, E., Charpentier, G., and Vachette, P. (2004) X-ray scattering study of pike olfactory nerve. II-Elastic, thermodynamic and physiological properties of the axonal membrane. *J. Mol. Biol.* **343,** 199–212.
7. Nagle, J. F. and Tristram-Nagle, S. (2000) Structure of lipid bilayers. *Biochim. Biophys. Acta - Rev. Biomembr.* **1469,** 159–195.
8. Helfrich, W. (1973) Elastic Properties of Lipid Bilayers—Theory and Possible. Experiments. *Z. Naturforsch. C.* **28,** 693–703.
9. Petrache, H. I., Gouliaev, N., Tristram-Nagle, S., Zhang, R. T., Suter, R. M, and Nagle, J. F. (1998) Interbilayer interactions from high-resolution x-ray scattering. *Phys. Rev. E* **57,** 7014–7024.
10. Parsegian, V. A., Rand, R. P., Fuller, N. L., and Rau, D. C. (1986) Osmotic-Stress for the Direct Measurement of Intermolecular Forces. *Methods Enzymol.* **127,** 400–416.
11. Parsegian, V. A., Rand, R. P., and Rau, D. C. (2000) Osmotic stress, crowding, preferential hydration, and binding: A comparison of perspectives. *Proc. Nat. Acad. Sci. USA* **97,** 3987–3992.
12. Parsegian, V. A., Rand, R. P., and Rau, D. C. (1995) Macromolecules and water: probing with osmotic stress. *Methods Enzymol.* **259,** 43–94.
13. Harries, D., Rau, D. C., and Parsegian, V. A. (2005) Solutes probe hydration in specific association of cyclodextrin and adamantane. *J. Am. Chem. Soc.* **127,** 2184–2190.
14. Bonnet-Gonnet, C., Leikin, S., Chi, S., Rau, D. C., and Parsegian, V. A. (2001) Measurement offerees between hydroxypropylcellulose polymers: Temperature favored assembly and salt exclusion. *J. Phys. Chem. B* **105,** 1877–1886.
15. Chik, J., Mizrahi, S., Chi, S. L., Parsegian, V. A., and Rau, D. C. (2005) Hydration forces underlie the exclusion of salts and of neutral polar solutes from hydroxypropylcellulose. *J. Phys. Chem. B.* **109,** 9111–9118.
16. Deme, B. and Zemb, T. (2000) Measurement of sugar depletion from uncharged lamellar phases by SANS contrast variation. *J. Appl. Crystallogr.* **33,** 569–573.
17. Mclntosh, T. J. and Simon, S. A. (1993) Contributions of hydration and steric (entropic) pressures to the interactions between phosphatidylcholine bilayers-Experiments with the subgel phase. *Biochemistry* **32,** 8374–8384.
18. Rau, D. C., Lee, B., and Parsegian, V. A. (1984) Measurement of the repulsive force between polyelectrolyte molecules in ionic solution: Hydration forces between parallel DNA double helices. *Proc. Nat. Acad. Sci. USA-Biol. Sci.* **81,** 2621–2625.

19. LeNeveu, D. M., Rand, R. P., and Parsegian, V. A. (1976) Measurement offerees between lecithin bilayers. *Nature* **259,** 601–603.
20. Mclntosh, T. J. (2000) Short-range interactions between lipid bilayers measured by X-ray diffraction. *Curr. Opin. Struct. Biol.* **10,** 481–485.
21. Leikin, S., Parsegian, V. A., Rau, D. C., and Rand, R. P. (1993) Hydration forces. *Annu. Rev. Phys. Chem.* **44,** 369–395.
22. Lyatskaya, Y., Liu, Y. F., Tristram-Nagle, S., Katsaras, J., and Nagle, J. F. (2001) Method for obtaining structure and interactions from oriented lipid bilayers. *Phys. Rev. E* **63,** 011907.
23. Parsegian, V. A., Fuller, N., and Rand, R. P. (1979) Measured work of deformation and repulsion of lecithin bilayers. *Proc. Nat. Acad. Sci. USA* **76,** 2750–2754.
24. Gawrisch, K., Ruston, D., Zimmerberg, J., Parsegian, V. A., Rand, R. P., and Fuller, N. (1992) Membrane dipole potentials, hydration forces, and the ordering of water a membrane surfaces. *Biophys. J.* **61,** 1213–1223.
25. Katsaras, J. (1998) Adsorbed to a rigid substrate, dimyristoylphosphatidylcholine multibilayers attain full hydration in all mesophases. *Biophys. J.* **75,** 2157–2162.
26. Kucerka, N., Liu, Y. F., Chu, N. J., Petrache, H. I., Tristram-Nagle, S. T., and Nagle, J. F. (2005) Structure of fully hydrated fluid phase DMPC and DLPC lipid bilayers using X-ray scattering from oriented multilamellar arrays and from unilamellar vesicles. *Biophys. J.* **88,** 2626–2637.
27. LeNeveu, D. M., Rand, R. P., Parsegian, V. A., and Gingell, D. (1977) Measurement and modification offerees between lecithin bilayers. *Biophys. J.* **18,** 209–230.
28. Lis, L. J., McAlister, M., Fuller, N., Rand, R. P., and Parsegian, V. A. (1982) Interactions between neutral phospholipid bilayer membranes. *Biophys. J.* **37,** 657–665.
29. McDaniel, R. V., Mclntosh, T. J., and Simon, S. A. (1983) Nonelectrolyte substitution for water in phosphatidylcholine bilayers. *Biochim. Biophys. Acta* **731,** 97–108.
30. Dubois, M., Zemb, T., Belloni, L., Delville, A., Levitz, P., and Setton, R. (1992) Osmotic pressure and salt exclusion in electrostatically swollen lamellar phases. *J. Chem. Phys.* **96,** 2278–2286.
31. Koynova, R. and Caffrey, M. (1998) Phases and phase transitions of the phosphatidylcholines. *Biochim. Biophys. Acta-Rev. Biomembr.* **1376,** 91–145.
32. Cevc, G. and Marsh, D. (1985) Hydration of noncharged lipid bilayer membranes. Theory and experiments with phosphatidylethanolamines. *Biophys. J.* **47,** 21–31.
33. Hauser, H., Paltauf, F., and Shipley, G. G. (1982) Structure and thermotropic behavior of phosphatidylserine bilayer membranes. *Biochemistry* **21,** 1061–1067.
34. Wiener, M. C., Tristram-Nagle, S., Wilkinson, D. A., Campbell, L. E., and Nagle, J. F. (1988) Specific volumes of lipids in fully hydrated bilayer dispersions. *Biochim. Biophys. Acta* **938,** 135–142.
35. Petrache, H. I., Kimchi, I., Harries, D., and Parsegian, V. A. (2005) Measured depletion of ions at the biomembrane interface. *J. Am. Chem. Soc.* **127,** 11,546–11,547.
36. Huang, T. C., Toraya, H., Blanton, T. N., and Wu, Y. (1993) X-ray powder diffraction analysis of silver behenate, a possible low-angle diffraction standard. *J. Appl. Crystallogr.* **26,** 180–184.
37. Lehninger, A. L. (1975) *Biochemistry,* Worth Publishers Inc., New York.
38. Porter, F. D. (2003) Human malformation syndromes due to inborn errors of cholesterol synthesis. *Curr. Opin. Pediatr.* **15,** 607–613.
39. Lis, L. J., McAlister, M., Fuller, N., Rand, R. P., and Parsegian, V. A. (1982) Measurement of the lateral compressibility of several phospholipid bilayers. *Biophys. J.* **37,** 667–672.
40. Petrache, H. I., Tristram-Nagle, S., Gawrisch, K., Harries, D., Parsegian, V. A., and Nagle, J. F. (2004) Structure and fluctuations of charged phosphatidylserine bilayers in the absence of salt. *Biophys. J.* **86,** 1574–1586.
41. Petrache, H. I., Harries, D., and Parsegian, V. A. (2004) Alteration of lipid membrane rigidity by cholesterol and its metabolic precursors. *Macromol. Symp.* **219,** 39–50.
42. Phillips, W. C. and Rayment, I. (1985) A systematic method for aligning double-focusing mirrors. *Methods Enzymol.* **114,** 316–329.